

Revenue Stacking of BESSs in Wholesale and aFRR Markets with Delivery Guarantees

Ángel Paredes , José A. Aguado 

Department of Electrical Engineering

University of Málaga

Málaga, Spain

{angelparedes, jaguado}@uma.es

Abstract—Battery Energy Storage Systems (BESSs) provide a crucial solution for mitigating the challenges posed by renewable energy intermittency, concurrently driving down energy costs within wholesale markets. To harness their potential, innovative business models are required for optimal BESS operation and revenue maximisation. This paper addresses this need by proposing a novel revenue stacking approach for the participation in Day-Ahead and automatic Frequency Restoration Reserve (aFRR) markets. By considering the uncertainty in the activation of aFRR events, the proposed model provides real-time delivery guarantees for a given reliability level, while maximising the revenues. The model is built over a novel characterisation of the uncertainty and a tight reformulation of the joint chance-constraints that drive energy and capacity guarantees. The effectiveness of the proposed approach is demonstrated through a case study based on real data from the Belgian market, yielding a 17.3% increase in profits over the individual chance-constraints approach.

Index Terms—aFRR, Joint Chance-Constraint, Revenue Stacking, Storage Systems, Uncertainty

I. INTRODUCTION

AS THE WORLD shifts to renewable energy sources, Battery Energy Storage Systems (BESSs) provide a promising solution to the challenge of intermittency and fluctuation of renewable generation for grid stability. Innovative business models are needed to capture the value of BESS services and incentive their deployment [1]. The increasing demand for sustainable energy and the need for efficient energy storage drive the exploration and optimization of BESS operations. The aim is to leverage the capabilities of BESSs to participate in multiple markets, and therefore maximise their profits [2]. These markets typically include wholesale and frequency restoration reserves. However, this capitalisation of the BESS capabilities is not straightforward, and it requires the development of new optimization techniques, and even new business models [3].

In this sense, authors in [4] propose a multi-service-based economic valuation of grid-connected BESSs procuring demand response and regulation services. Reference [5] explores revenue stacking for behind-the-meter BESSs inside of local energy systems participating in wholesale and ancillary services markets, through a linear cost-minimisation optimization problem. However, only behind-the-meter applications were considered. To overcome this issue, reference [6] introduces an optimization framework for dynamic multi-use applications that considers both behind and front-the-meter applications for multiple power and energy capacity allocations. Authors in [7] propose a bi-level model for BESSs participating in national day-ahead markets and local flexibility markets. Nevertheless, these works do not consider the uncertainty in the operation of the BESS.

To address this challenge, several techniques have been proposed in the literature. A risk-aware technique is proposed in [8] to optimize the reserve scheduling of BESSs for active distribution networks, based on a two-stage model. Multi-stage robust and stochastic optimization are used by [9] for the participation of BESSs in local energy markets. In [10], short-term power fluctuations are considered in the scheduling of BESSs for a frequency-constrained energy management strategy in energy islands. A nested multi-scale dynamic programming approach is proposed in [11] for BESSs operating in wholesale and frequency regulation markets, considering the uncertainty in the load demand, electricity prices and regulation signals. Besides of this, [12] proposes a scenario-based risk evaluation associated to the uncertainty of renewable energy and electricity prices. Reference [13] proposes a dynamic programming approach to optimize the scheduling of electric buses, considering the uncertainty associated to the battery capacity fading. However, challenges related to computational complexity and scalability of scenario-based approaches may limit their real-world applicability.

To overcome these limitations, reference [14] proposes a control policy that maximise market benefits, considering the uncertainty in the battery degradation and the penalties for not meeting the market requirements through a chance-constrained optimization problem. However, the uncertainty in the activation of the automatic Frequency Restoration Reserve (aFRR) events is not considered. This is addressed by [15] through a detailed characterization of the duration of the

Submitted to the 23rd Power Systems Computation Conference (PSCC 2024). Á. Paredes and J. A. Aguado work was supported by the FPU grant (FPU19/03791) founded by the Spanish Ministry of Education, by Ministerio de Ciencia e Innovación through project TED2021-132339B-C42, by Horizon Europe Programme through project HORIZON-CL5-2022D3-01 Ref: 101096787 and, by the University of Málaga. The authors thankfully acknowledge the computer resources provided by the SCBI center of the University of Málaga.

aFRR events, which is then used to ensure real-time delivery guarantees using Individual Chance Constraints (ICCs). Nevertheless, Transmission System Operators (TSOs) rarely activate all power capacity of the BESS in a single event and the direction could change at any moment during the delivery. Considering both facts within the same chance-constraint is a challenging task that has not been addressed in literature and has the potential to unlock new revenue streams.

The aforementioned studies have demonstrated the potential of BESSs to provide multiple services and maximise revenue. However, there are still research gaps that need to be addressed. First, new characterisations of the activation of the aFRR events that maximise the use of the BESS capabilities and provide real-time delivery guarantees are needed. This is of overwhelming importance for this market, specially in the case of stacking of multiple services. An accurate representation of the uncertainty of the activation unlocks hidden operation strategies that maximise the utilisation of BESSs. Thus, this ultimately lead to an increase in their suitability to stack multiple services and benefits. Besides, taking into account these characteristics is crucial to provide real-time delivery guarantees, which require Joint Chance Constraints (JCCs) to be considered.

These topics have not been properly discussed in literature. In order to address these limitations, this paper proposes a novel optimization framework for the revenue stacking of BESSs in the Day-Ahead Market (DAM) and aFRR markets considering bid activation. The methodology considers the uncertainty associated to the delivery of the aFRR products, both in energy and power dimensions using a tight convex reformulation of the JCC. Note that, in the proposed model, penalties for the energy not delivered are excluded from the objective function, addressed through the JCC reformulation and the BESS operator's choice of reliability level. The key feature is that the proposed model provides real-time delivery guarantees for a given reliability level, while maximising the revenue in the operation. The contributions of this paper are summarised as follows:

- C1 A methodology for revenue stacking of BESSs in DAM and aFRR markets is presented. This approach leverages a novel characterization of the activation of aFRR events in both energy and power dimensions, derived from historical data. Specifically, the characterization encompasses the duration and activation ratio of aFRR events, streamlining the representation of the market dynamics and providing real-time guarantees.
- C2 A convex reformulation of the JCC, which enable a tighter representation of the reliability level. This allows the benefits of BESSs to be leveraged in the aFRR market, while providing real-time delivery guarantees.

The remainder of the paper is structured as follows. Section II presents the problem formulation and the methodology. Then, case study is presented in section III. Finally, section IV concludes the paper.

II. PROBLEM FORMULATION AND METHODOLOGY

In this section, the problem is formulated and the proposed methodology for the revenue stacking of BESSs in the DAM and aFRR markets is presented. The hereby methodology is based on the following assumptions:

- A1 The operation strategy is decided before the clearing of the DAM and the aFRR clearing, i.e. DAM prices λ_t^{DAM} , the clearing reserve λ_t^u , and λ_t^d and energy $\lambda_t^{aFRR,u}$ and $\lambda_t^{aFRR,d}$ prices of the aFRR market are forecast [16]. A clear timeline of the proposed methodology is shown in Fig. 1. These bids consider the probability of the activation during the next day, if an unforeseen situation occurs, the BESS operator can modify the operation strategy in intra-day markets, but this is out of the scope of this paper.
- A2 Joint participation in the DAM and aFRR markets is allowed. Based on this, the BESS can be used to provide aFRR services, while participating in the DAM market as long as the battery is not charged and discharged at the same time.
- A3 Upward and downward aFRR activation are statistically coupled, i.e. the probability of an upward activation is dependent of the probability of a downward activation. This assumption is supported by the evidence drawn for the statistical analysis of the delivery of the events, and further discussed in section II-A.

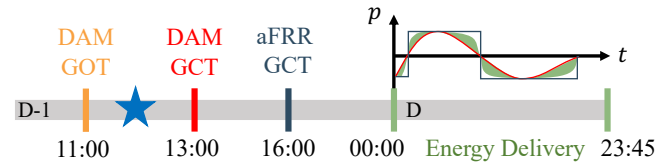


Fig. 1: Timeline of the proposed methodology. The BESS is scheduled in the DAM and aFRR markets in a day-ahead basis before DAM Gate Closing Time (GTC). Then, the BESS is deliver energy products in real-time.

Before delving into the details of the problem formulation, the main characteristics of the aFRR market are investigated.

A. aFRR market characterization

Automatic frequency restoration services are defined in two stages, namely capacity contract and activation. The first is defined in a day-ahead market-based auction, where the TSO contracts the required power capacity for the next day in an hourly basis. Then, the TSO activates the contracted power capacity in real-time, in response to a frequency deviation. This activation might be partial and is linked to a market clearing of the balancing energy among the previous summited capacity contracts [17]. Thus, it is possible to characterise this activation in terms of the overall balancing energy that is activated, as shown in Fig. 2.

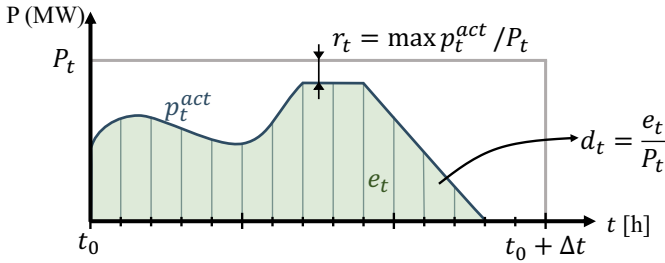


Fig. 2: Shape of an aFRR event. Activated p_t^{act} and contracted P_t power are represented by blue and grey lines, respectively. The energy of the event e_t is in green area. Duration d_t and ratio of activation r_t are visualised in the figure.

Let p_t^{act} and P_t be the activated and contracted aFRR power at time t , an event is characterized by its duration d_t and the ratio of activation r_t , which are defined as:

$$d_t = \frac{1}{P_t} \int_{t_0}^{t_0 + \Delta t} p_t^{act} dt \quad \forall t_0 \quad (1a)$$

$$r_t = \max\{p_t^{act}\}_{t_0}^{t_0 + \Delta t} / P_t \quad \forall t_0 \quad (1b)$$

Here, t_0 is the time of activation of the event, and Δt is the duration of the contracted services, i.e. 15 minutes. Note that the computation of these magnitudes needs a high resolution of p_t^{act} , i.e. 1-minute data for this case. These two parameters are crucial to characterize aFRR events, and therefore they are used in the proposed model.

However, the ratio of activation and the duration of the events are magnitudes that are correlated, as Fig. 3 (a) and (b) depicts. Besides, as shown in the histogram of Fig. 3 (c) and (d), there is an inverse correlation between the duration of the activation of upward and downward events. This means that a change in direction of the aFRR event is likely to occur in the middle of a period, which makes the characterization of the aFRR events more challenging. This is captured by the proposed model through a joint statistical characterization of the duration and ratio parameters. Their joint dependence is modelled by the JCCs presented in the next section.

B. Uncertainty-aware revenue stacking model

The characterization of the aFRR events presented in the previous section is used to develop a novel revenue stacking model for BESSs in the DAM and aFRR markets.

The BESS sells p_t^s and buys p_t^b power in the DAM market at time t , and provide upward $p_t^{ch,u}$, $p_t^{dis,u}$ and downward $p_t^{ch,d}$, $p_t^{dis,d}$ aFRR services, i.e. the BESS is discharged more or charged less to provide upward services, and vice versa for downward services. Binary variable z_t indicates the charging of the BESS, soc_t , soc_t^{aFRR} are the state of charge in DAM and aFRR considering efficiencies η_t^{ch} and η_t^{dis} for charging and discharging, and upper and lower \overline{SOC} , \underline{SOC} limits. Note that State of Charge (SOC) is considered as an uncertain variable depending on the realisation of the activation of the aFRR event. \overline{P} is the power of the converter and Δt is the time step of the markets. The reliability level α is assumed

to be the same for power and energy constraints in the aFRR market. In addition, the level α^{TGT} indicates the reliability of the target of energy at the end of the scheduling horizon $\|\Omega_t\|$. Lastly, to account for the degradation of the BESS, a semi-empirical model is used to compute the degradation of the battery as the sum of its calendar $\Delta b_{loss,t}^{cal}$ and cycle $\Delta b_{loss,t}^{cyc}$ degradation. The calendar degradation is expressed as a function of the target SOC soc_t^{TGT} , and the cycle degradation is expressed as a function of the C_{rate} , i.e. the ratio of the charging and discharging power to the power of the converter. $\Delta b_{loss,t}^{cal}(soc_t^{TGT})$ and $\Delta b_{loss,t}^{cyc}(C_{rate})$ are non-linear functions which are discretized in m segments and interpolated as linear functions with parameters a_m , b_m , c_m , and d_m [18], [19]. To penalize the degradation, the degradation cost C^{DEG} is included in the objective function as the unitary cost of replacement of the battery. This will avoid the overuse of the BESS for those cases when the profits are not enough to cover the degradation costs. The proposed optimization model is formulated as follows:

$$\begin{aligned} \max \quad & \sum_t \lambda_t^{DAM} (p_t^s - p_t^b) + \sum_t [\lambda_t^u (p_t^{ch,u} + p_t^{dis,u}) + \\ & + \lambda_t^d (p_t^{dis,d} + p_t^{ch,d})] + \sum_t [\lambda_t^{aFRR,u} (p_t^{dis,u} - p_t^{ch,u}) d_t^u + \\ & + \lambda_t^{aFRR,d} (p_t^{dis,d} - p_t^{ch,d}) d_t^d - C^{DEG} (\Delta b_{loss,t}^{cal} + \Delta b_{loss,t}^{cyc})] \end{aligned} \quad (2a)$$

Subject to,

$$soc_t = soc_{t-1} + \eta_t^{ch} p_t^{ch} \Delta t - \frac{p_t^{dis}}{\eta_t^{dis}} \Delta t \quad \forall t > 0 \quad (2b)$$

$$\underline{SOC} \leq soc_t \leq \overline{SOC} \quad \forall t \quad (2c)$$

$$\mathcal{P} \left\{ \begin{array}{l} p_t^b + p_t^{ch,d} r_t^d - p_t^{ch,u} r_t^u \leq \overline{P} z_t \\ p_t^b + p_t^{ch,d} r_t^d \leq \overline{P} z_t \\ p_t^b - p_t^{ch,u} r_t^u \geq 0 \\ p_t^s + p_t^{dis,u} r_t^u - p_t^{dis,d} r_t^d \leq \overline{P} (1 - z_t) \\ p_t^s + p_t^{dis,u} r_t^u \leq \overline{P} (1 - z_t) \\ p_t^s - p_t^{dis,d} r_t^d \geq 0 \end{array} \right\} \geq 1 - \alpha \quad \forall t \quad (2d)$$

$$\begin{aligned} soc_t^{aFRR} = soc_{t-1}^{aFRR} + \left[\left(\eta_t^{ch} p_t^b - \frac{p_t^s}{\eta_t^{dis}} \right) \Delta t + \left(\eta_t^{ch} p_t^{ch,d} + \right. \right. \\ \left. \left. + \frac{p_t^{dis,d}}{\eta_t^{dis}} \right) d_t^d - \left(\eta_t^{ch} p_t^{ch,u} + \frac{p_t^{dis,u}}{\eta_t^{dis}} \right) d_t^u \right] \quad \forall t \quad (2e) \end{aligned}$$

$$\mathcal{P} \{ \underline{SOC} \leq soc_t^{aFRR} \leq \overline{SOC} \} \geq 1 - \alpha \quad \forall t \quad (2f)$$

$$\mathcal{P} \{ soc_{\|\Omega_t\|}^{aFRR} \geq SOC^{TGT} \} \geq 1 - \alpha^{TGT} \quad (2g)$$

$$p_t^{ch,u} + p_t^{dis,u} \geq P^{MIN} y_t^u \quad \forall t \quad (2h)$$

$$p_t^{ch,d} + p_t^{dis,d} \geq P^{MIN} y_t^d \quad \forall t \quad (2i)$$

$$p_t^{ch,u} + p_t^{dis,u} \leq M y_t^u \quad \forall t \quad (2j)$$

$$p_t^{ch,d} + p_t^{dis,d} \leq M y_t^d \quad \forall t \quad (2k)$$

$$\Delta b_{loss,t}^{cal} \geq a_m soc_t^{TGT} + b_m \quad \forall m, \forall t \quad (2l)$$

$$\Delta b_{loss,t}^{cyc} \geq c_m (p_t^{ch} - p_t^{dis}) / P^{conv} + d_m \quad \forall m, \forall t \quad (2m)$$

The objective function (2a) maximises the stacked revenues in the DAM and aFRR markets considering that the cost of aFRR energy is the same as the DAM energy. Degradation costs are also considered in the objective function, where $\Delta b_{loss,t}^{cal}$ and $\Delta b_{loss,t}^{cyc}$ are the calendar and cycle degradation at time t , respectively. Equations (2b) and (2c) compute the SOC of the BESS, while (2e) computes the SOC of the BESS in the aFRR market. Then, the JCC (2d) ensures that the BESS is able to provide the contracted aFRR power capacity, while the JCC (2f) ensures that the SOC of the BESS is within the limits during the aFRR operation, at least $1 - \alpha$ of the time. Besides, the JCC (2g) ensures that the SOC of the BESS is above the target SOC at the end of the time horizon $\|\Omega_t\|$. Note that α^{TGT} is typically bigger than α , as the target SOC is a less restrictive constraint than the SOC limits, because of the economic penalties associated to the Balancing Energy Not Delivered (BEND). The JCCs are the key feature of the proposed model, as they enable the provision of real-time delivery guarantees for a given reliability level $1 - \alpha$. Additionally, in most reserve markets, minimum bids P^{MIN} are required to be submitted. These are enforced by (2h) to (2k), for upward and downward directions, respectively. Note that y_t^u and y_t^d are binary variables that indicate the activation of the upward and downward events, respectively, and M is a large number. Battery degradation is computed as the sum of the cycle and calendar degradation (2l) and (2m), respectively. The economic ageing model is obtained from [18], where the parameters a_m, b_m, c_m, d_m are interpolated from calendar and cycle degradation curves [19] for each segment m .

C. Convex reformulation of the JCCs

The JCC (2d), (2f) and (2g) are not suitable for direct resolution by commercial solvers. To overcome this, the JCCs are reformulated as a set of ICCs with more restrictive individual reliability levels α_j . These levels are traditionally computed based on Boole's inequality [20], which states that the probability of meeting a set of constraints $g_j(x, \xi) \leq 0$ with $j \in \Omega_j$ is lower than the sum of the probability of meeting each constraint $g_j(x, \xi) \leq 0$ individually, i.e.:

$$\mathcal{P}\{g_j(x, \xi) \leq 0, \forall j\} \leq \sum_{j \in \Omega_j} \mathcal{P}\{g_j(x, \xi) \leq 0\} \quad (3a)$$

In other words, $\alpha \geq \sum_{j \in \Omega_j} \alpha_j$. Considering that the level of reliability of the JCC is set to $1 - \alpha$, the most conservative approach is to set the probability of meeting each constraint individually to $\alpha_j = \alpha / \|\Omega_j\|$. However, this approach tends to over-count the intersection of the events, which leads to ex-post probability violations lower than the desired level of reliability. To deal with this concern, a tighter representation of α_j is used, based on reference [21]. The joint probability $\mathcal{P}\{g_j(x, \xi) > 0\}$ is estimated derived from Monte Carlo simulations, which is then used to tighten the level of reliability $1 - \alpha_j$ for each constraint. Then, the confidence level for each constraint is set to:

$$\alpha_j = \frac{\alpha + \mathcal{P}\{g_j(x, \xi) > 0\}(\|\Omega_j\| - 1)}{\|\Omega_j\|} \quad \forall j \quad (3b)$$

The joint probability $\mathcal{P}\{g_j(x, \xi) > 0\}$ is approximated as:

$$\mathcal{P}\{g_j(x, \xi) > 0\} = \frac{\sum_{m=1}^{N_m} 1_{(g_j(x, \xi) > 0 \forall j)}}{N_m} \quad \forall j \quad (3c)$$

being m the index of the Monte Carlo simulation, and N_m the number of simulations, sampled from the joint distribution of the random parameters ξ . The number of required samples N_m is computed as [22]:

$$N_m \geq \frac{2}{\alpha} \left(\ln \frac{1}{\beta} + N_d \right) \quad (3d)$$

where N_d is the number of decision variables, and β is the confidence level of the approximation, typically selected to 99%. For the case at hand, the JCCs aim to provide real-time delivery guarantees for power and energy variables, over a time horizon $t \in \Omega_t$, then $N_d = 2|\Omega_t|$. Then, the JCC is reformulated as a set of ICCs (3e), where the level of reliability α_j is computed using (3b) and (3c).

$$\mathcal{P}\{g_j(x, \xi) \leq 0\} \geq \alpha_j \quad \forall j \in \Omega_j \quad (3e)$$

Obtaining tight values for the individual confidence levels α_j , the ICCs are reformulated using their deterministic equivalent based on the quantiles of the random parameters ξ , with $\phi_\xi^-(\varepsilon)$ the ε -quantile of the distribution of ξ , i.e. $\phi_\xi^-(\varepsilon) = \inf\{y \in \mathbb{R}^+ : \mathcal{P}(\xi \leq y) \geq \varepsilon\}$.

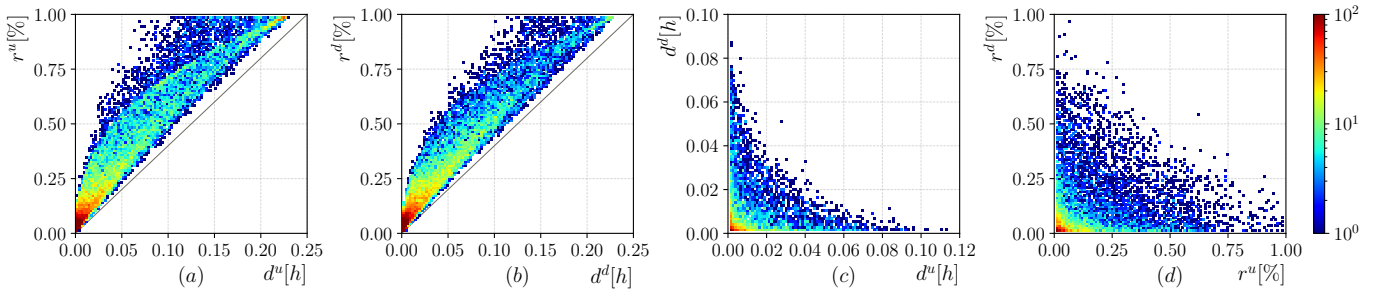


Fig. 3: 2D Histogram of the correlation between the ratio of activation r_t and the duration d_t in upward (a) and downward (b) directions, and between the duration (c) and ratio of activation (d) of upward and downward events occurring in the same period t . The colour represents the number of events.

JCCs are reformulated as a set of ICCs (3e), which are then reformulated as a deterministic equivalent based on the quantiles of the random parameters ξ . The deterministic equivalent of the JCCs (2d), (2f) and (2g), based on individual reliability levels $\alpha_1, \alpha_2, \dots, \alpha_8$ are computed as:

$$p_t^b + p_t^{ch,d} \phi_{r_t^d}^-(\alpha_1) - p_t^{ch,u} \phi_{r_t^u}^-(1 - \alpha_1) \leq \bar{P}z_t \quad \forall t \quad (4a)$$

$$p_t^b + p_t^{ch,d} \phi_{r_t^d}^-(1 - \alpha_2) \leq \bar{P}z_t \quad \forall t \quad (4b)$$

$$p_t^b - p_t^{ch,u} \phi_{r_t^u}^-(1 - \alpha_3) \geq 0 \quad \forall t \quad (4c)$$

$$p_t^s + p_t^{dis,u} \phi_{r_t^u}^-(\alpha_4) - p_t^{dis,d} \phi_{r_t^d}^-(1 - \alpha_4) \leq \bar{P}(1 - z_t) \quad \forall t \quad (4d)$$

$$p_t^s + p_t^{dis,u} \phi_{r_t^u}^-(1 - \alpha_5) \leq \bar{P}(1 - z_t) \quad \forall t \quad (4e)$$

$$p_t^s - p_t^{dis,d} \phi_{r_t^d}^-(1 - \alpha_6) \geq 0 \quad \forall t \quad (4f)$$

$$\begin{aligned} \underline{SOC} \leq & SOC0 + \sum_{t=t_0}^t \left[\left[\eta^{ch} p_t^b - \frac{p_t^s}{\eta^{dis}} \right] \Delta t + \left[\eta^{ch} p_t^{ch,d} + \right. \right. \\ & \left. \left. \frac{p_t^{dis,d}}{\eta^{dis}} \right] \phi_{d_t^d}^-(\alpha_7) - \left[\eta^{ch} p_t^{ch,u} + \frac{p_t^{dis,u}}{\eta^{dis}} \right] \phi_{d_t^u}^-(1 - \alpha_7) \right] \quad \forall t \quad (4g) \end{aligned}$$

$$\begin{aligned} \overline{SOC} \geq & SOC0 + \sum_{t=t_0}^t \left[\left[\eta^{ch} p_t^b - \frac{p_t^s}{\eta^{dis}} \right] \Delta t + \left[\eta^{ch} p_t^{ch,d} + \right. \right. \\ & \left. \left. \frac{p_t^{dis,d}}{\eta^{dis}} \right] \phi_{d_t^d}^-(1 - \alpha_8) - \left[\eta^{ch} p_t^{ch,u} + \frac{p_t^{dis,u}}{\eta^{dis}} \right] \phi_{d_t^u}^-(\alpha_8) \right] \quad \forall t \quad (4h) \end{aligned}$$

$$\begin{aligned} SOC^{TGT} \leq & SOC0 + \sum_{t=t_0}^{\|\Omega_t\|} \left[\left[\eta^{ch} p_t^b - \frac{p_t^s}{\eta^{dis}} \right] \Delta t + \left[\eta^{ch} p_t^{ch,d} + \right. \right. \\ & \left. \left. \frac{p_t^{dis,d}}{\eta^{dis}} \right] \phi_{d_t^d}^-(\alpha^{TGT}) - \left[\eta^{ch} p_t^{ch,u} + \frac{p_t^{dis,u}}{\eta^{dis}} \right] \phi_{d_t^u}^-(1 - \alpha^{TGT}) \right] \quad (4i) \end{aligned}$$

Therefore, the optimization problem becomes a MILP, which can be solved using off-the-shelf solvers. It maximises (2a) subject to equations (2b) – (2c), (2l), (2m) and (4a) – (4i). Note that the problem is solved twice; in the first iteration, $\alpha_j = \alpha$, which gives an initial schedule used to compute the joint probability $P\{g_j(x, \xi) \geq 0\}$ using (3c). Then, the level of probability is tightened using (3b), and the problem is solved again to obtain the final schedule.

In this section, the proposed methodology is demonstrated through a case study based on real data from the Belgian market. Wholesale market prices and aFRR market prices can be found in [23], while minute resolution data of the aFRR events can be found in [24]. The case study is based on a BESS with 2 MW of power capacity and 10 MWh of energy capacity, which is connected to the Belgian aFRR market. The charging and discharging efficiencies are set to 0.95 and 0.92, respectively. For a time horizon of 24 hours with 15 minutes resolution, and a confidence level $1 - \alpha$ of 98%, the number of required samples for the JCC reformulation is $N_m = 19,202$. The optimization problem is solved using Pyomo 6.5 [25] over Python 3.9.15 and Gurobi 10.0.1 [26] in a computer with an Apple M1 3.2 GHz processor and 16 GB of RAM. The problem has 1,442 constraints, 769 continuous and 288 binary variables, and it is solved in 0.2692 seconds with a MIP gap of 0.01%. To evaluate the probability of meeting the JCCs, 30,000 samples are generated using the joint quantile function of the random parameters. It takes 8.34 seconds to generate the samples, and 9.76 seconds to evaluate them.

A. Revenue stacking in the DAM and aFRR markets

The BESS stacks revenues from DAM and aFRR markets by leveraging the ability of the battery to provide multiple services simultaneously. Representative price profiles for λ_t^{DAM} , λ_t^{aFRR} , λ_t^u and λ_t^d are generated based on data from 2022. DAM and upward aFRR product prices lie between 250 and 400 €/MW, while downward aFRR around 20 to 50 €/MW. The revenue stacking of the different products is depicted in Fig. 4 (a). Energy trading in DAM is piled with products from aFRR between 12:00 and 21:00 for this case study. In light of the product prices, BESS maximise the revenues with upward aFRR products by discharging the battery while selling DAM energy, as seen in Fig. 4 (c). The energy drawn in these operations are obtained by buying DAM energy whenever the λ_t^{DAM} is forecasted to be lower than λ_t^u , as Fig. 4 (b) shows. Due to the characterisation of the aFRR events and the JCCs, the battery submits offers bigger than the total capacity of the battery, in anticipation of not being fully activated, to maximise the profits, as Fig. 4 (c) shows.

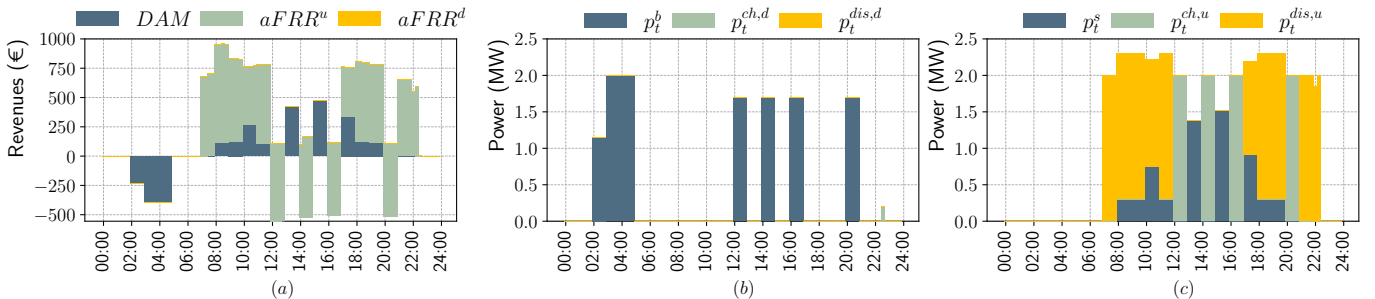


Fig. 4: Stacked revenue of the BESS in the DAM and aFRR markets. (a) Stacked revenues, (b) Charging products, (c) Discharging products.

The revenues obtained in the markets strongly depends on the level of reliabilities α and α^{TGT} considered. The less strict the JCCs are, the more revenues are possible to obtain from DAM and aFRR participation. Nevertheless, this comes at the cost of not delivering all the energy that the TSO eventually activates. The overall reliability, BEND, and the expected profits can be computed in an ex-post analysis, for a given pair (α, α^{TGT}) . Figure 5 shows that there is a non-linear relationship between the α, α^{TGT} and the magnitudes at hand. Overall, the less strict the JCCs are, the higher the revenues are, but with higher BEND. Thus, a trade-off must be selected between these parameters depending on the penalties the regulator will declare for not delivering the balancing energy, since the relationship between the BEND and the reliability levels (α, α^{TGT}) is non-linear. Note that the BESS operator could eventually select a pair $(\alpha = 50\%, \alpha^{TGT} = 10\%)$ with negligible BEND and 40 k€ of profits, or a pair $(\alpha = 15\%, \alpha^{TGT} = 50\%)$ obtaining similar results depending on how the BEND is penalised and operational restrictions over targeted SOC.

B. Tightening the reliability level

To showcase how the proposed strategy tighten the reliability of the JCCs, the ex-post uncertainty level for equations (4a) to (4i) for three different approaches to solve the market bidding problem are compared. The first approach separates the JCCs and solve the resulting ICCs using univariate quantiles of the stochastic parameters $r_t^u, r_t^d, d_t^u,$ and d_t^d . Then, as the proposed methodology relies on a two-step process to solve the JCCs, resulting uncertainty levels for each step, i.e. Boole's rule and the improved case, are computed and compared in Table I for the case of α and α^{TGT} being 2% and 20%, respectively. The first approach is overly conservative, leading to a null uncertainty level, which means that no constrain violation occur, although 2% is allowed by the BESS operator.

Then, the improved case enables higher uncertainty level for (2f) than using the traditional Boole's rule. This fact unlocks profits as shown in Table II, being able to obtain 17.3% more of profits compared to the ICCs approach and unlocking 5.08% of profits compared to the Boole's rule through a more aggressive strategy in the DAM.

To exemplify this behaviour, Fig. 6 is plotted for the three different approaches comparing the final schedule for the BESS in the DAM p_t^{DAM} and aFRR p_t market if the capacity product is fully activated. Fig. 6 (a) shows that the bidding strategy when solving univariate ICCs will not exceed the converter capacity, neglecting what the data indicates about the actual activation of the products. This results in a strict bidding strategy which foresee full bid activations which might not happen when the uncertainty is realised, as the ex-post reliability analysis demonstrated. Then, Fig. 6 (b) and Fig. 6 (c) shows the bidding strategy for the Boole's rule and the improved case, where the BESS operator over-contract the battery in expectancy of a partial activation as the data indicates. The final quantity of products p_t obtained using Boole's rule is close to the actual value of P^{conv} between 08:00 to 12:00 and 17:00 to 20:00, compared to the improved case. In addition, the amount of upward product offered between 20:00 and 22:30, increases. This is due to the tightening of the reliability level which, in practice, assumes that the duration of the event will be shorter, so it can send bigger bids.

C. Impact of the degradation of the battery

The previous sections demonstrated the effectiveness of the proposed method to increase benefits exploiting the flexibility potential of the BESS in DAM and aFRR markets. Still, this increase in C-rate and SOC activity must be balanced with an adequate level of wear. To do so, a linearized degradation model for the cycle and calendar ageing is used. The degradation cost C^{DEG} is computed as the investment cost

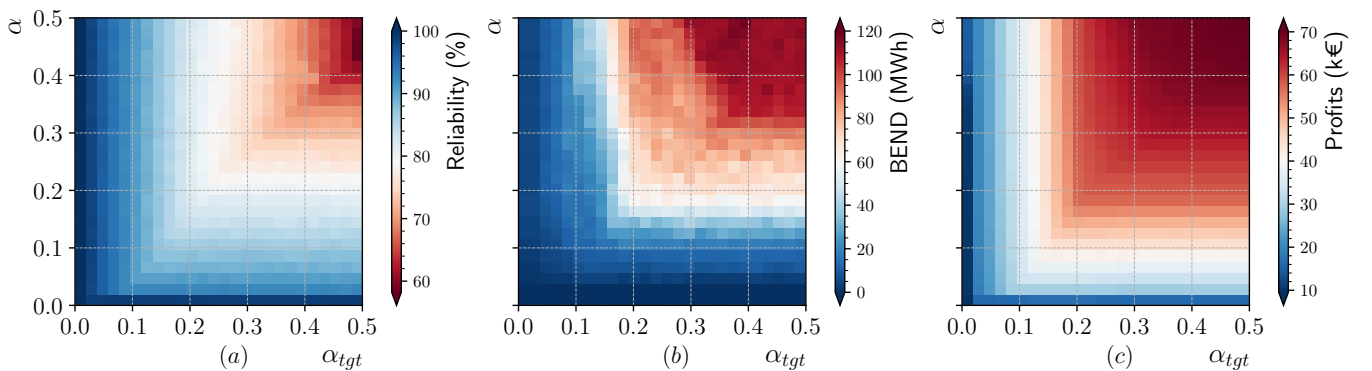


Fig. 5: Reliability analysis for different levels of α and α^{TGT} . (a) Ex-post reliability, (b) BEND, (c) Profits in the markets.

TABLE I: Comparison of the ex-post uncertainty level using ICCs, Boole's rule and the improved approach to obtain α_j .

	(4a)	(4b)	(4c)	(4d)	(4e)	(4f)	(4g)	(4h)	(4i)	(2d)	(2f)
ICCs	0%	0%	0%	0%	0%	0%	0%	0%	0.015%	0%	0%
Boole's	0%	0%	0.373%	0.373%	0.373%	0%	1.065%	0.028%	8.183%	0.373%	1.093%
Improved	0%	0%	0.383%	0.383%	0.383%	0%	1.056%	0.025%	7.96%	0.383%	1.083%
Asking α	2%	2%	2%	2%	2%	2%	2%	2%	20%	2%	2%

TABLE II: Comparison of the revenues obtained using ICCs approach, Boole's rule and the Improved Case.

	DAM Buy	DAM Sell	aFRR Upward	aFRR Downward	Total
ICCs	- 8,662.88 €	4,828.75 €	12,931.26 €	- 1.92 €	9,095.21 €
Boole's	- 12,432.08 €	7,636.71 €	15,242.51 €	- 8.24 €	10,438.90 €
Improved	- 12,538.00 €	8,301.41 €	15,242.51 €	- 8.24 €	10,997.69 €
ICCs vs Improved	30.91%	41.83%	15.16%	76.67%	17.30%
Boole's vs Improved	0.84%	8.01%	0.00%	0.00%	5.08%

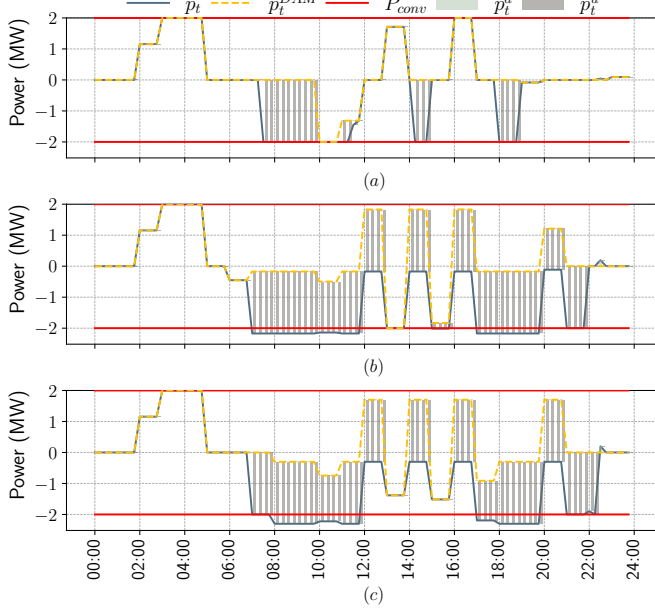


Fig. 6: Schedule for the BESS for the three different approaches to solve the BESS market bidding problem. p_t^{DAM} indicates the DAM schedule, p_t indicates the aFRR schedule assuming full bid activation, P^{CONV} shows the converter limits, while p_t^u and p_t^d shows the upward and downward aFRR contracted products for (a) ICCs, (b) Boole's equation, (c) improved case.

of the battery I divided by the total energy loss at the end of its lifetime $1 - SOH_{EOL}$, i.e. $C^{DEG} = I / (1 - SOH_{EOL})$, where SOH_{EOL} is the state of health at the end of its lifetime. For this case study, the investment cost is assumed to be 200 €/kWh, while SOH_{EOL} is set to 60% [18], calendar and cycle degradation curves are fitted using a set of $m = 10$ segments.

The scheduling difference between a degradation-aware and free model is presented in Fig. 7, where it can be seen that the degradation-aware (yellow lines) model tends to reduce the level of SOC of the battery compared to the degradation-free modelling (blue lines), while opting for aFRR (dashed lines) products before charging DAM (solid lines) products. This can be seen at 07:00 and at 18:00 in Fig. 7 (a), where the degradation-aware scheduling opt for discharging the battery to reduce the DAM and target SOC, as shown in Fig. 7 (b). Under these conditions, an increase of 2.14% in the energy sold to the DAM is observed during the day. The DAM and targeted SOC levels are reduced 0.67% and

0.73%, respectively compared to the degradation-free model. The total costs of the degradation add up to 250.69€ for a volume of 34,161.34€ of stacked profits in the markets, which represents 0.73% of the total. However, a reduction of 0.96% of the objective arises between the degradation-free and degradation-aware models, meaning that the degradation phenomena reduces by 0.23% the total revenues obtained in the day, but increasing the lifetime of the battery.

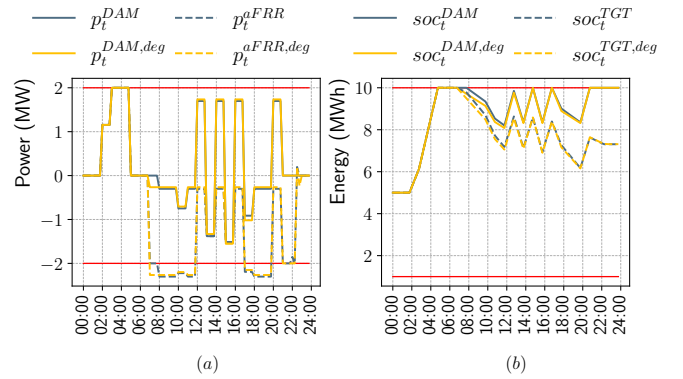


Fig. 7: Comparison of the power (a) and SOC (b) with and without degradation-aware scheduling. Blue lines represent the case without degradation, while yellow lines represent the case with degradation. Dashed lines indicate aFRR scheduling while solid lines indicate DAM scheduling.

IV. CONCLUSION

This paper has presented a BESS scheduling methodology for maximising the revenue in DAM and aFRR markets, considering the uncertain nature of the activation of the aFRR products. The proposed optimization problem took into account the intrinsic characteristics of the aFRR activation events by describing them using the ratio of activation and the duration of the event. Introducing these magnitudes, along with a tight resolution of the JCCs, leverages the BESS capabilities to provide the services and maximise the stacked benefits. The problem addressed partial activation of the products based on one year data obtained from the Belgian market, which increases the profits BESSs obtain from their participation.

A convex and tight reformulation of the JCCs enables a fast computation of the MILP model, taking under 1 minute for the whole procedure. The level of reliability is tightened based on an ex-post analysis of the joint probability of not meeting the constraints. This method unlocks market revenues by relaxing the α values of the equivalent ICCs, resulting in a 17.3% increase in profits in this case study, tightening the

real reliability to the required by the JCCs. In addition, the impact of the degradation of the battery is analysed based on a segmentation of the calendar and cycle ageing curves. In essence, the SOC levels are reduced to reduce calendar wear, by increasing the amount of discharging products offered to the market. Under 0.5% reduction in profits is observed in the degradation-aware model for the daily schedule, which is remunerated in the long-term by an extended lifetime of the battery. The effectiveness of the proposed model is also guaranteed after the integration into the PICASSO platform, since no significant changes in the activation profiles are expected. Nevertheless, further research should be conducted to confirm this statement once the platform is operational.

REFERENCES

- [1] N. Brinkel, M. Zijlstra, R. van Bezu, T. van Twuijver, I. Lampropoulos, and W. van Sark, "A comparative analysis of charging strategies for battery electric buses in wholesale electricity and ancillary services markets," *Transp. Res. Part E Logist. Transp. Rev.*, vol. 172, p. 103085, 2023.
- [2] A. Ramos, M. Tuovinen, and M. Ala-Juusela, "Battery Energy Storage System (BESS) as a service in Finland: Business model and regulatory challenges," *J. Energy Storage*, vol. 40, 2021.
- [3] J. Martins and J. Miles, "A techno-economic assessment of battery business models in the UK electricity market," *Energy Policy*, vol. 148, p. 111938, 2021.
- [4] S. Yamujala, A. Jain, R. Bhakar, and J. Mathur, "Multi-service based economic valuation of grid-connected battery energy storage systems," *J. Energy Storage*, vol. 52, p. 104657, 2022.
- [5] W. Seward, M. Qadrdan, and N. Jenkins, "Revenue stacking for behind the meter battery storage in energy and ancillary services markets," *Electr. Power Syst. Res.*, vol. 211, p. 108292, 2022.
- [6] S. Englberger, A. Jossen, and H. Hesse, "Unlocking the Potential of Battery Storage with the Dynamic Stacking of Multiple Applications," *Cell Reports Phys. Sci.*, vol. 1, p. 100238, 2020.
- [7] K. Steriotis, K. Sepetanc, K. Smpoukis, N. Efthymiopoulos, P. Makris, E. Varvarigos, and H. Pandzic, "Stacked Revenues Maximization of Distributed Battery Storage Units Via Emerging Flexibility Markets," *IEEE Trans. Sustain. Energy*, vol. 13, pp. 464–478, 2022.
- [8] X. Li, X. Han, and M. Yang, "Risk-Based Reserve Scheduling for Active Distribution Networks Based on an Improved Proximal Policy Optimization Algorithm," *IEEE Access*, vol. 11, pp. 15 211–15 228, 2023.
- [9] D. Badanjak and H. Pandzic, "Battery Storage Participation in Reactive and Proactive Distribution-Level Flexibility Markets," *IEEE Access*, vol. 9, pp. 122 322–122 334, 2021.
- [10] S. Córdova, C. A. Cañizares, Á. Lorca, and D. E. Olivares, "Frequency-Constrained Energy Management System for Isolated Microgrids," *IEEE Trans. Smart Grid*, vol. 13, pp. 3394–3407, 2022.
- [11] B. Cheng and W. B. Powell, "Co-Optimizing Battery Storage for the Frequency Regulation and Energy Arbitrage Using Multi-Scale Dynamic Programming," *IEEE Trans. Smart Grid*, vol. 9, pp. 1997–2005, 2018.
- [12] K. Pandzic, K. Bruninx, and H. Pandzic, "Managing Risks Faced by Strategic Battery Storage in Joint Energy-Reserve Markets," *IEEE Trans. Power Syst.*, vol. 36, pp. 4355–4365, 2021.
- [13] J. Wang, L. Kang, and Y. Liu, "Optimal scheduling for electric bus fleets based on dynamic programming approach by considering battery capacity fade," *Renew. Sustain. Energy Rev.*, vol. 130, p. 109978, 2020.
- [14] B. Xu, Y. Shi, D. S. Kirschen, and B. Zhang, "Optimal battery participation in frequency regulation markets," *IEEE Trans. Power Syst.*, vol. 33, pp. 6715–6725, 2018.
- [15] J. F. Toubeau, J. Bottieau, Z. De Greeve, F. Vallee, and K. Bruninx, "Data-Driven Scheduling of Energy Storage in Day-Ahead Energy and Reserve Markets with Probabilistic Guarantees on Real-Time Delivery," *IEEE Trans. Power Syst.*, vol. 36, pp. 2815–2828, 2021.
- [16] L. Baringo and A. J. Conejo, "Offering strategy via robust optimization," *IEEE Trans. Power Syst.*, vol. 26, pp. 1418–1425, 2011.
- [17] European Network of Transmission System Operators for Electricity (ENTSOE), "aFRR & IN Optimisation Mathematical Description for Publication," Tech. Rep., 2022. [Online]. Available: https://eepublicdownloads.blob.core.windows.net/public-cdn-container/clean-documents/Network%20codes%20documents/NC%20EB/2022/20220406_PICASSO_Public_Algorithm_description_v1.0.pdf
- [18] N. Collath, B. Tepe, S. Englberger, A. Jossen, and H. Hesse, "Aging aware operation of lithium-ion battery energy storage systems: A review," *J. Energy Storage*, vol. 55, no. PC, p. 105634, 2022.
- [19] M. A. Ortega-Vazquez, "Optimal scheduling of electric vehicle charging and vehicle-to-grid services at household level including battery degradation and price uncertainty," *IET Gener. Transm. Distrib.*, vol. 8, no. 6, pp. 1007–1016, 2014.
- [20] G. Boole, *An Investigation of the Laws of Thought on Which Are Founded the Mathematical Theories of Logic and Probabilities*, T. M. Press, Ed. Dover Publications, New York, NY, 1958.
- [21] K. Baker and B. Toomey, "Efficient relaxations for joint chance constrained AC optimal power flow," *Electr. Power Syst. Res.*, vol. 148, pp. 230–236, 2017.
- [22] M. C. Campi, S. Garatti, and M. Prandini, "The scenario approach for systems and control design," *Annual Reviews in Control*, vol. 33, pp. 149–157, 2009.
- [23] ENTSO-E, "ENTSO-E Transparency Platform," 2022. [Online]. Available: <https://transparency.entsoe.eu/transmission-domain/r2/dayAheadPrices/show?areaType=BZN>
- [24] ELIA Group, "ELIA Grid Data," 2022. [Online]. Available: www.elia.be/en/grid-data/data-download
- [25] W. E. Hart, J.-P. Watson, D. L. Woodruff, and J. D. Siirola, *Pyomo - Optimization Modeling in Python*, 2nd ed. Cham, Switzerland: Springer International Publishing, 2017.
- [26] Gurobi Optimization, LLC, "Gurobi Optimizer Reference Manual," 2023. [Online]. Available: <https://www.gurobi.com>